

## ADSORPTION AND CONDENSATION OF XANTHINE AT THE MERCURY/SOLUTION INTERFACE

Viktor DRAZAN<sup>a,l</sup> and Vladimir VETTERL<sup>a,b,\*</sup>

<sup>a</sup> Institute of Biophysics, Academy of Sciences of the Czech Republic, 612 65 Brno, Czech Republic;

e-mail: <sup>1</sup>vdrazan@ipb.cz

<sup>b</sup> Department of Physical Electronics, Faculty of Science, Masaryk University, 611 37 Brno,

Czech Republic; e-mail: vetterl@ipb.cz

Received February 3, 1998

Accepted August 7, 1998

The adsorption and two-dimensional condensation of xanthine at the mercury electrode in 0.2 and 2 M NaCl was studied by electrode double layer capacity measurements. The condensation of xanthine molecules adsorbed at the electrode was observed at pH 6.0 and 7.4, but not at 9.0. The standard Gibbs energy of adsorption, energy of lateral interactions and the surface occupied by one xanthine molecule in a compact layer were calculated from the temperature dependence of the capacity pit using the Frumkin and Ising lattice gas models. The orientation of xanthine molecules in a compact layer at the electrode surface was estimated. At higher bulk concentrations of xanthine, the double layer capacity decreases to a very low value of about  $1.5 \mu\text{F cm}^{-2}$ , which might be an indication of the formation of a xanthine multilayer at the electrode surface.

**Key words:** Adsorption of purine bases; Frumkin adsorption isotherm; Electrochemical impedance; Ising model; Mercury/aqueous interface; Xanthine; Electrochemistry; Purines.

In our previous studies, we found that the bases (and most nucleosides) usually occurring in nucleic acids can undergo a two-dimensional (2-D) condensation at the mercury electrode surface resulting in the formation of a compact surface film. In the range of potentials at which the surface film is formed, the differential capacity of the electrode double layer is considerably depressed, giving rise to characteristic "pits" on capacity-potential ( $C-E$ ) curves<sup>1-4</sup>. Retter has shown that the adsorption energy and energy of interaction between molecules forming the compact layer as well as the area occupied by one molecule in the compact layer can be calculated from the temperature dependence of the pit width<sup>5-7</sup>.

We observed earlier that those purine and pyrimidine derivatives which are not usually present in nucleic acids (like isocytosine, xanthine, hypoxanthine) did not form

\* The author to whom correspondence should be addressed: Institute of Biophysics, Academy of Sciences of the Czech Republic, 612 65 Brno, Czech Republic.

a compact film on the mercury dropping electrode unlike currently occurring bases (adenine, thymine, guanine, cytosine, uracil) under the otherwise same experimental conditions<sup>1,2</sup>. The reasons for this are not yet known.

In order to clear up this problem, we have studied the adsorption of xanthine at the mercury drop electrode with the aim to find out whether the experimental conditions can be found at which the 2-D condensation of xanthine can be observed. In the present paper we show that the 2-D condensation of xanthine can be observed at pH 6.0 (neutral xanthine) and pH 7.4 but not at pH 8.5 and higher, when most of xanthine molecules carry negative electric charges. We have calculated the surface occupied by one molecule in the compact layer and the adsorption and interaction energies.

## EXPERIMENTAL

The background electrolyte was 0.2 or 2 M NaCl prepared from Merck analytical grade NaCl, treated with activated charcoal overnight, then filtered through a fine (S4) sintered glass frit. Xanthine (Fluka puriss., Lot No. 199345378) was used as received. Xanthine solutions were prepared by dissolution at a higher temperature (about 100 °C), subsequent cooling to room temperature and filtering off the precipitate. All xanthine solutions and supporting electrolytes were stored in a refrigerator at 5 °C. Before every measurement, the solution was heated in a boiling-water bath to dissolve the precipitated xanthine. pH of the samples was adjusted using 1 M HCl and 1 M NaOH (analytical grade). The stability of pH adjusted in this way was sufficient for our measurements in order to secure an unchanged degree of xanthine ionization during the measurement. Some measurements were performed in 2 M NaCl with a Britton–Robinson (BR) buffer. The concentration of the buffer was half of the tabulated values (BR/2). The concentration of xanthine was determined from the UV absorbance using molar absorption coefficients given in literature<sup>8</sup>. All measurements were made with solutions deaerated using 99.5% argon saturated with triple distilled water. The water used was distilled in a glass electrodistillator followed by double distillation in quartz.

The measurement of the electrode impedance was performed using an AUTOLAB electrochemical system (Ecochemie, Utrecht, Netherlands) equipped with a potentiostat/galvanostat PGStat20 and a frequency-response analyzer (FRA) module at the following settings (if not otherwise stated): frequency 225 Hz, AC voltage amplitude 0.5 mV, integration time 0.2 s, the number of cycles to reach steady state 50.

The measured values of the electrode double layer impedance can be expressed using the AUTOLAB/FRA software as the resistance  $R_s$  and capacity  $C_s$  of an equivalent circuit consisting of a resistor and a capacitor connected in series. This simple equivalent circuit can be used only in the potential range where no electrode reaction takes place<sup>9</sup> and/or no dielectric losses in the adsorption–desorption process are involved. The measurement of the electrode double layer impedance in the frequency range 20–2 000 Hz has shown that with the xanthine solutions the serial equivalent circuit can be used in the potential range, where the 2-D condensation has been observed.

The working electrode was a mercury drop electrode Metrohm 663 VA Stand, operating either as a hanging (HMDE) or a static (SMDE) mercury drop electrode. In the HMDE mode, the mercury drop was dispensed at the starting potential and the measurement in the whole potential scan was performed with this single drop. In the SMDE mode, each point of measurement is made with a new drop. The drop area  $S = 0.0034 \text{ cm}^2$  (position 2 on the 663 VA stand) was determined by weighing one hundred droplets.

In the SMDE mode, the single and/or double potential step technique was used. The new drop was dispensed at the potential of  $-1.75$  or  $-1.85$  V, at which the electrode surface is supposed to be free from adsorbed molecules. The electrode was held at this potential for 1 s. Then the electrode potential was switched either to the measurement potential (single step technique) or to the potential of maximum adsorption (hereinafter denoted as the adsorption potential) and – after adsorption – to the measurement potential (double step technique). The adsorption potential in double step technique was chosen close to the potential of zero charge of the supporting electrolyte. The time of adsorption ( $t_p$ ) in double step technique and the time of equilibration on the measurement potential in both techniques were determined from the time dependence of the electrode-double-layer capacity (see  $C-t$  curves, Fig. 4) as the time at which the formation of the compact layer is finished and the double layer capacity does not change with time any longer. The  $C-t$  curves were measured for each xanthine concentration at the highest temperature at which the pit still appears; here the 2-D condensation is slowest. The electrode was held for 1 s at a potential of  $-1.7$  V before each  $C-t$  measurement. Continuous stirring with a mechanical stirrer during the pretreatment and measurement accelerates the attainment of equilibrium values of the electrode-double-layer impedance so that lower value of  $t_p$  can be used.

The reference electrode was a saturated calomel electrode (SCE) Radelkis OP-0830F. This electrode was connected to the measured solution through a salt bridge with a Vycor® frit, filled with the background electrolyte. Platinum wire was used as an auxiliary electrode. The temperature was controlled by a cryostat with the accuracy of  $\pm 0.5$  °C. The thermostated polarographic vessels were home-made.

## RESULTS AND DISCUSSION

### *Dependence on pH and NaCl Concentration*

We have tried to find out whether by changing the pH value or NaCl concentration of the xanthine solutions, such conditions can be reached under which the 2-D condensation of xanthine molecules at the electrode surface can be observed. The  $pK$  value of the deprotonation of xanthine is 7.4 (refs<sup>8,10</sup>). We have measured xanthine solutions at three different pH values. At pH 6.0 most xanthine molecules in the solution are without an electric charge, at pH =  $pK$  = 7.4 about 50% of the molecules are neutral and the rest are negatively charged, at pH 8.5–9.0 most of the xanthine molecules are deprotonated and carry negative charges.

If the 2-D condensation of adsorbed xanthine molecules takes place, there should appear “pits” on the  $C-E$  curves. The pits measured with HMDE usually show a hysteresis, *i.e.*, the range of potentials in which the pit occurs depends on the direction and speed of the potential scan<sup>5,11–13</sup>.

No pits were observed with xanthine solutions measured at pH 9.0 at room (Fig. 1) or at low temperatures (not shown), even at xanthine concentrations approaching the saturation value (0.35 mmol  $l^{-1}$  in 0.2 M NaCl and 1.1 mmol  $l^{-1}$  in 2 M NaCl at 25 °C). A small dependence of the  $C-E$  curves on the direction of the potential scan is observed (Fig. 1, curves 1, 2). When the scan from  $-0.05$  to  $-1.8$  V is used (Fig. 1, curve 2), anions of the supporting electrolyte specifically adsorbed at the electrode surface can be pres-

ent<sup>14–16</sup>. The adsorbed anions can cause an increase in the double-layer capacity value and the curve 2 has thus around –0.5 V higher  $C_s$  values than the curve 1. The increase in the double layer capacity due to adsorption of charged molecules has been observed by Miller with ionized polyacids<sup>17</sup>. A sharp peak near –0.15 V is obviously caused by a Faradayic process. At this potential, deprotonized xanthine forms an insoluble compound with mercury as was described earlier by Paleček<sup>19</sup> and Ibrahim *et al.*<sup>20</sup>. This compound can hinder the adsorption of xanthine and increase the capacity value around –0.5 V if the scan from positive to negative potentials is used (Fig. 1, curve 2). If the opposite direction of the potential scan is applied (curve 1), xanthine molecules are adsorbed on a clean electrode surface, neither supporting electrolyte ions nor electrode reaction products participating in the adsorption, and the double layer capacity around –0.5 V is lower than it was with curve 2. At potentials more positive than –0.15 V, the insoluble compound which is formed at –0.15 V blocks the electrode surface and decreases considerably the capacity value (Fig. 1, curve 1).

In the potential range from –0.4 to –0.9 V the  $C_s$  values, measured in xanthine solution with SMDE (Fig. 1, curve 3), are slightly higher than the values measured with HMDE (Fig. 1, curves 1, 2). The adsorption rate in 0.68 mM xanthine solution is slow and, unlike with HMDE, the adsorption equilibrium is not reached with SMDE using the equilibration time 3 s. The 2-D condensation is not observed at pH 9.0 due to the negative charge of the adsorbed xanthine molecules which prevents their closer contact at the electrode surface.

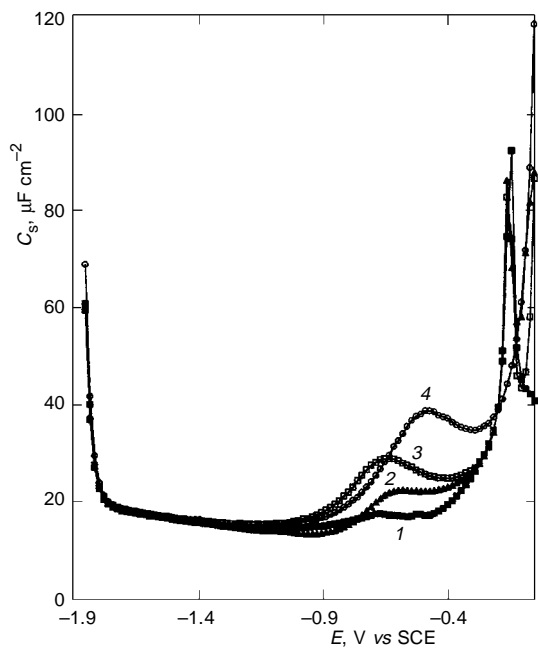


FIG. 1  
 $C-E$  curves for 0.68 mM xanthine in 2 M NaCl at pH 9.0 and 25 °C. HMDE, scan from: 1 –1.85 to –0.05 V; 2 –0.05 to –1.85 V; 3, 4 SMDE (single-step technique,  $t_p = 3$  s); 4 supporting electrolyte

Contrary to the measurements performed at pH 9.0, the 2-D condensation of xanthine molecules was observed at pH 6.0 and 7.4, when most (pH 6) or some (pH 7.4) of xanthine molecules in the solution are neutral. A well-defined pit appears on the  $C-E$  curves of 0.68 mM xanthine in 2 M NaCl at these pH values (Fig. 2, curves 2 and 3). Similarly Ahmed *et al.*<sup>21</sup> have found that xanthine forms capacity pits at pH 3.2 and 7.2 but not at pH 9.2. Rueda *et al.*<sup>22</sup> have found that hypoxanthine forms capacity pits at pH 5.0 when almost only neutral hypoxanthine molecules are in the solution. At pH 2.0 when both protonated and neutral forms exist in the solution, no pits were observed<sup>22</sup>.

When the double-step technique is used with SMDE, the differential capacity is lowered in a wide potential range (Fig. 2, curve 1) showing that the electrode is covered by a layer of xanthine molecules. An "enhanced adsorption" occurs as it will be discussed later.

To avoid the effect of buffer ions on the 2-D condensation of nucleic acid bases and nucleosides, some authors prefer working without buffer, as it was done in the studies of 2-D condensation of thymine in 1 M NaCl (ref.<sup>12</sup>), uracil in 0.4 M Na<sub>2</sub>SO<sub>4</sub> (ref.<sup>23</sup>), uridine in 0.5 M Na<sub>2</sub>SO<sub>4</sub> (refs<sup>23,24</sup>) and adenosine in 0.5 M Na<sub>2</sub>SO<sub>4</sub> (ref.<sup>25</sup>).

### Enhanced Adsorption

Figure 3 shows the dependence on the xanthine concentration of the  $C-E$  curves measured with SMDE in 2 M NaCl at pH 6 without buffer. The measurements were

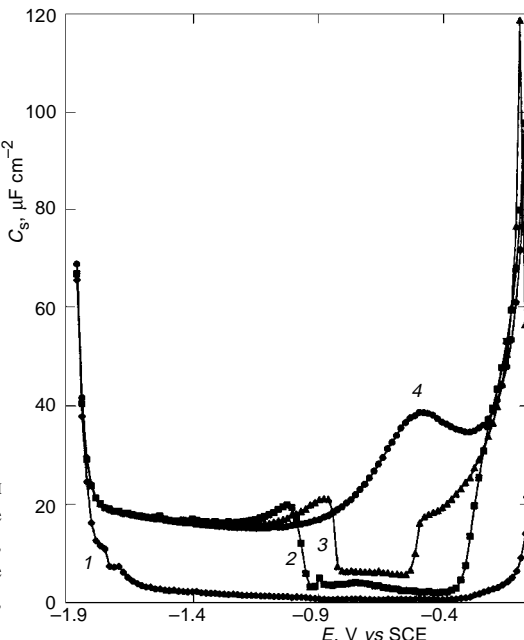


FIG. 2  
 $C-E$  curves for 0.68 mM xanthine in 2 M NaCl (1, 2, 3) and supporting electrolyte (4) at pH 6.0 (1, 2, 4) and 7.4 (3), SMDE, 25 °C. Measurement technique: 1 double step; 2, 3, 4 single step.  $t_p$  (s): 1 10; 2, 3, 4 3

performed using the double-step technique, the adsorption and equilibration times  $t_p$  being 10 s. The 2-D condensation and compact monolayer formation take place in the concentration range of 0.07–0.14 mmol  $l^{-1}$ . In this range, the pit width increases with increasing concentration very little and the pit bottom capacity remains unchanged.

At xanthine concentrations 0.28 mmol  $l^{-1}$  and higher (Fig. 3, curves 1–3) the adsorption and condensation potential regions become wider, the capacity decreasing down to a value of about 1.5  $\mu F \text{ cm}^{-2}$ . The  $C-E$  curves of xanthine solutions are below the values of the background electrolyte almost in the whole potential range, *i.e.*, up to about –1.8 V. Thus, the layer of adsorbed xanthine molecules remains at the electrode surface even at quite negative potentials, at which the electrode is negatively charged; usually, the adsorbed neutral molecules are expelled from the electrode surface at negative potentials by the electrostatically attracted cations of the supporting electrolyte<sup>12,15,27</sup>.

Earlier, we have observed a similar effect of enhanced adsorption with adenine at low temperatures<sup>4</sup>. We have explained this behaviour by the formation of a multilayer and/or a layer composed of adenine with incorporated cations which enable the compact layer to cover the electrode surface even if the electrode is negatively charged.

#### Time Dependence of the Electrode Double Layer Impedance ( $C-t$ Curves)

The 2-D condensation is a nucleation and growth process. The time dependence of the double layer capacity during this process has an S-shaped form<sup>4,12,13,15,28</sup>. Such a course

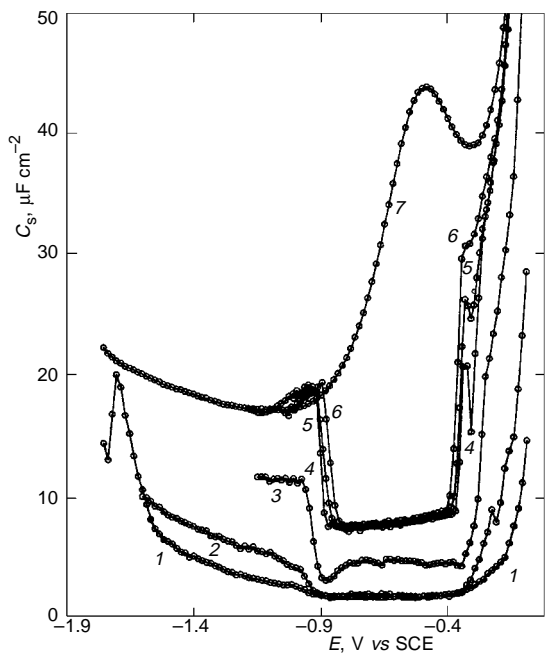


FIG. 3  
 $C-E$  curves for xanthine in 2 M NaCl at pH 6.0 and 20 °C. SMDE, using the double-step technique,  $t_p = 10$  s. Dependence on xanthine concentration  $c$  (mmol  $l^{-1}$ ): 1 1.1, 2 0.55, 3 0.28, 4 0.14, 5 0.13, 6 0.07, 7 0 (20 °C, HMDE, scan from –0.05 to –1.85 V)

of  $C-t$  curves was observed with 0.13 mM xanthine in 2 M NaCl (pH 6.0) at 30 and 35 °C (Fig. 4, curves 4–7). At 23 °C (curve 3), the rate of 2-D condensation is so high that the capacity  $C_s$  corresponding to the completely covered surface is reached already within 3 s after the application of potential step, when the first point of the  $C-t$  curve in Fig. 5 was measured.

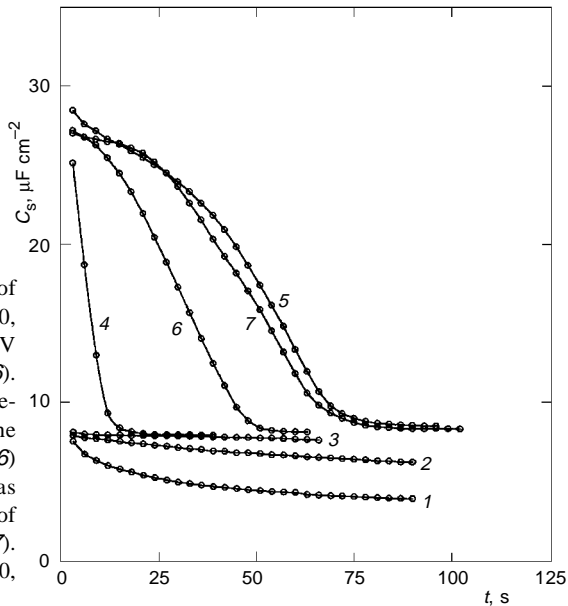
At 20 °C, the double layer capacity starts further to decrease below the value  $C_s$  of the pit bottom (Fig. 4, curve 2) corresponding to the formation of a multilayer of xanthine molecules and/or a layer containing xanthine and ions of the basic electrolyte, as was discussed in previous section. At still lower temperatures (curve 1), a further decrease in the capacity is observed, which might be caused by an increase in the coverage degree and/or thickness of the second-type layer due to the adsorption of further xanthine molecules.

The rate of 2-D condensation depends not only on temperature but also on the electrode potential. The highest rate of condensation is observed at the potential of maximum adsorption  $E_m$ . Comparing curves 5 and 6 in Fig. 4, it can be judged that the potential  $-0.6$  V (curve 6) is closer to the potential  $E_m$  than the potential  $-0.56$  V (curve 5). If the electrode potential was not switched before the  $C-t$  measurement to the desorption potential of  $-1.7$  V and held there for 1 s, then the rate of condensation was higher (curve 7) than if desorption preceded the  $C-t$  measurement (curve 5).

On the basis of the  $C-t$  curves measured, the adsorption and equilibration time  $t_p = 10$  s was chosen. From Fig. 4 it follows that during this time the formation of the compact

FIG. 4

Temperature dependence of  $C-t$  curves of 0.13 mM xanthine in 2 M NaCl at pH 6.0, measured at the potential of  $-0.55$  V (curves 1–5, 7) and at  $-0.60$  V (curve 6). Before the measurement of the time dependence, the Hg electrode was at the desorption potential  $-1.7$  V (curves 1–6) held for 1 s or the measurement was started immediately after the application of the corresponding potential (curve 7). Temperature (°C): 1 17, 2 20, 3 23, 4 30, 5 35, 6 35, 7 35



monolayer at the potential  $-0.55$  V was finished in a  $0.13$  mM xanthine solution at  $20$  and  $23$   $^{\circ}\text{C}$  (Fig. 4, curves 2 and 3). Thus the pit bottom capacity,  $C_m = 7.5 \mu\text{F cm}^{-2}$ , of curves 4–6 in Fig. 3 is an equilibration value. The pit bottom capacity of xanthine approaches the value observed with other nucleic acid bases forming the compact layers (adenine  $6.1 \mu\text{F cm}^{-2}$  (refs<sup>4,8</sup>), cytosine  $5.5 \mu\text{F cm}^{-2}$  (refs<sup>2,26</sup>)).

#### *Measurements with the Hanging Mercury Drop Electrode (HMDE)*

Figure 5 shows the effect of the direction of the electrode potential scan on the  $C$ – $E$  curves measured with the HMDE. It can be seen that the pit of  $0.07$  mM xanthine (Fig. 5, curves 3 and 4) shows a pronounced hysteresis. The capacity value of the pit bottom minimum  $7.5 \mu\text{F cm}^{-2}$  is the same as with SMDE (Fig. 3).

At higher xanthine concentrations (Fig. 5, curves 1 and 2), the potential range of adsorption and condensation becomes wider, and the capacity decreases down to a value of about  $1.5 \mu\text{F cm}^{-2}$ , similarly to what was observed using SMDE (Fig. 3). By the potential scan from negative to positive potentials (curve 2), the condensation starts at  $-1.08$  V (negative pit edge), and at  $-1.4$  V the electrode surface is not covered by xanthine. By opposite scan (curve 1) the electrode surface is at  $-1.4$  V still covered. It means that at  $-1.4$  V the electrode is covered by the xanthine layer only if previously stays at some potentials more positive than  $-1.1$  V. This was also shown in Fig. 2 – the adsorption at  $-1.4$  V takes place only if the double-step technique is used.

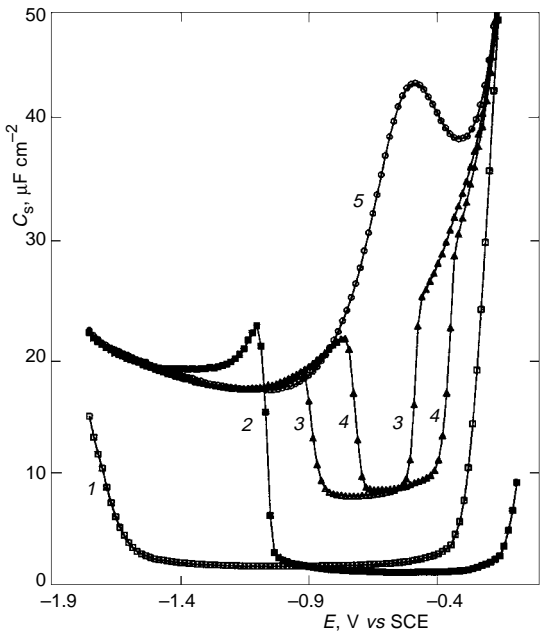


FIG. 5  
 $C$ – $E$  curves for xanthine in  $2$  M  $\text{NaCl}$  at  $\text{pH} 6.0$  and  $20$   $^{\circ}\text{C}$ . Dependence on xanthine concentration  $c$  and potential scan direction, HMDE. Concentration  $c$  ( $\text{mmol l}^{-1}$ ): 1, 2  $1.1$ ; 3, 4  $0.07$ ; 5  $0$ . Scan direction: 1, 3, 5 from  $-0.05$  to  $-1.85$  V; 2, 4 from  $-1.85$  to  $-0.05$  V

### The Temperature Dependence of Adsorption

Figures 6 and 7 show the temperature dependencies of the pit widths measured with SMDE from which the adsorption parameters were calculated (see the next section). In 0.2 M NaCl (Fig. 6), the adsorption time used ( $t_p = 6$  s) was lower than in 2 M NaCl ( $t_p = 10$  s, Fig. 7) because the establishment of the 2-D condensation equilibrium – the formation of the compact layer – is faster in 0.2 than in 2 M NaCl (  $C$ - $t$  curves measured in 0.2 M NaCl are not shown). The pit width is larger in 0.2 than in 2 M NaCl.

### Calculation of Adsorption Parameters

The dependence of the pit width on temperature can be described<sup>5</sup> by the equation

$$(E_h - E_m)^2 = K_1 T + K_2 , \quad (1)$$

where

$$K_1 = 2 R \Gamma_m \ln (c/c_0)/(C_0 - C_s) \quad (2)$$

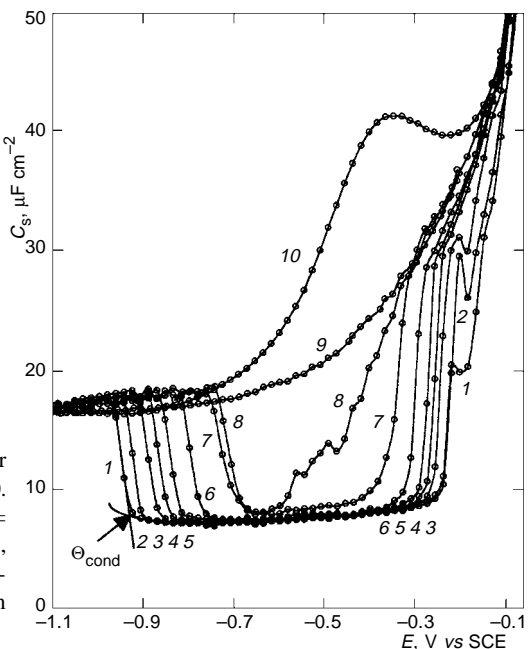


FIG. 6

Temperature dependence of  $C$ - $E$  curves for 0.11 mM xanthine in 0.2 M NaCl at pH 6.0. SMDE, using the double-step technique,  $t_p = 6$  s. Temperature (°C): 1 17, 2 20, 3 23, 4 25, 5 27, 6 30, 7 33, 8 34, 9 35, 10 supporting electrolyte at 20 °C (HMDE, scan from -0.05 to -1.85 V)

and

$$K_2 = -2 \Gamma_m (\Delta G^m + a') / (C_0 - C_s) . \quad (3)$$

In these equations,  $E_m$  is the potential of the adsorption maximum,  $E_h$  the potential of the capacity pit edge, *i.e.*, the potential at which the degree of coverage of the electrode by a compact film  $\Theta_f$  equals 0.5.  $\Gamma_m$  is the possible maximum surface concentration;  $C_0$  and  $C_s$  are the capacities of the double layer of the free and completely covered ( $\Theta_f = 1$ ) electrode surface;  $c$  and  $c_0$  are the molar concentrations of solute (xanthine) and solvent (for aqueous solvent  $c_0 = 55.5 \text{ mol l}^{-1}$ , molar concentration of water).  $\Delta G^m$  is the standard Gibbs energy of adsorption at  $E = E_m$ ;  $a'$  is the lateral interaction energy between adsorbed molecules, related to the lateral interaction coefficient  $a$  of the Frumkin adsorption isotherm

$$a = -a'/RT . \quad (4)$$

(The temperature dependence of  $a'$  is not taken into consideration in Eqs (2) and (3).) According to Eq. (1), the plot of  $(E_h - E_m)^2$  versus  $T^{-1}$  should be a straight line. From the slope  $K_1$  and section  $K_2$ , the possible maximum surface concentration,  $\Gamma_m$ , and the

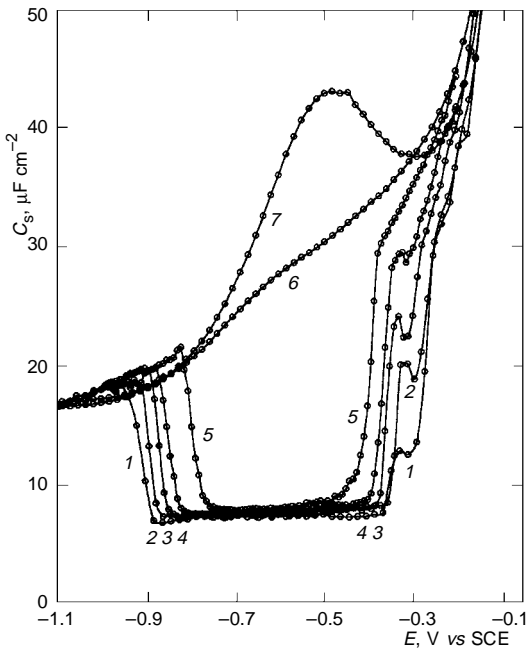


FIG. 7  
Temperature dependence of  $C$ - $E$  curves for 0.13 mm xanthine in 2 M NaCl at pH 6.0. SMDE, using the double-step technique,  $t_p = 10$  s. Temperature (°C): 1 17, 2 20, 3 25, 4 27, 5 30, 6 40 (HMDE, scan from -0.05 to -1.85 V), 7 supporting electrolyte at 20 °C (HMDE, scan from -0.05 to -1.85 V)

sum of energies,  $\Delta G^m + a'$ , can be calculated. The separate determination of the lateral interaction energy  $a'$  alone can be made if the capacitance pit bottom has a "ramp-like" shape<sup>6</sup>. In this case the capacity  $C_{\text{cond}}$  and the coverage degree  $\Theta_{\text{cond}}$  can be estimated, corresponding to the potential at which the compact film ruptures and an abrupt increase in the double layer capacity (pit edge) follows (see Fig. 6). The lateral interaction energy  $a'$  can then be determined from the measured  $\Theta_{\text{cond}}$

$$\Theta_{\text{cond}} = (C_{\text{=}} - C_{\text{cond}})/(C_{\text{=}} - C_{\text{s}}) , \quad (5)$$

where  $C_{\text{=}}$  is the capacity of the upper part of the pit edge (where the compact layer is destroyed and the electrode is covered by flat-adsorbed xanthine molecules), and  $C_{\text{s}}$  is the capacity of the pit bottom (the electrode is completely covered by the compact layer).

The calculation of the interaction energy  $a'$  and/or the interaction parameter  $a$  (Eq. (4)) from the measured value of  $\Theta_{\text{cond}}$  depends on the theoretical adsorption model used. According to the Frumkin model<sup>5</sup>,

$$a = a_F = [\ln(1 - \Theta_{\text{cond}}) - \ln \Theta_{\text{cond}}]/(1 - 2 \Theta_{\text{cond}}) . \quad (6)$$

For the two-dimensional lattice gas (Ising) model, we obtain<sup>6</sup>

$$a = a_G = 4 \operatorname{arcsinh} X = 4 \ln(X + (X^2 + 1)) , \quad (7)$$

$$X = [1 - (2 \Theta_{\text{cond}} - 1)^8]^{-1/4} . \quad (8)$$

If it is experimentally possible to determine the value  $C_{\text{cond}}$  not only for one temperature but for several ones, then the temperature dependence of the interaction parameter  $a$  can be followed. The interaction parameter  $a$  increases with decreasing temperature<sup>6</sup> according to the equation

$$a = K_3/T + K_4 , \quad (9)$$

where

$$K_3 = a_c(1 + b)T_c , \quad (10)$$

$$K_4 = -a_c b . \quad (11)$$

With decreasing temperature, the interaction parameter  $a$  increases and at temperatures lower than *condensation temperature*,  $T_{\text{cond}}$ , the condensation of adsorbed molecules starts to appear. The condensation temperature,  $T_{\text{cond}}$ , depends on the concentration of xanthine and is higher with increasing xanthine concentration. The dependence of  $1/T_{\text{cond}}$  on  $\ln(c)$  should be a straight line<sup>8</sup>. The *critical temperature*,  $T_c$ , is the highest possible condensation temperature and, unlike the condensation temperature  $T_{\text{cond}}$ , it does not depend on the concentration  $c$  of adsorbate in the solution<sup>8</sup>. At a critical temperature  $T_c$ , the interaction parameter  $a$  reaches the critical value  $a_c$ . For the Frumkin adsorption model,  $a_c = a_{Fc}$ , where

$$a_{Fc} = 2 \quad (12)$$

and for lattice-gas model,  $a_c = a_{Gc}$ , where

$$a_{Gc} = 4 \operatorname{arcsinh}(1) = 3.525\dots \quad (13)$$

$a_c$  corresponding in both models to  $\Theta_{\text{crit}} = 0.5$  (*i.e.*,  $X = 1$  in the lattice-gas model).

When it was experimentally found that the temperature dependence of the interaction coefficient  $a'$  must be taken into consideration, more general equations for  $K_1$  and  $K_2$  were used instead of Eqs (2) and (3) (ref.<sup>6</sup>):

$$K_1 = 2 R \Gamma_m [\ln(c/c_0) + a'_c b/RT_c]/(C_0 - C_s) , \quad (14)$$

$$K_2 = -2 \Gamma_m (\Delta G^m + a'_c (1 + b))/(C_0 - C_s) , \quad (15)$$

where

$$a' = a'_c [1 + b(T_c - T)/T_c] , \quad (16)$$

$$a'_c = -a_c RT_c . \quad (17)$$

(Equations (14) and (15) become identical with Eqs (2) and (3) for  $b = 0$ .)

Table I summarizes the calculated values of surface concentration  $\Gamma_m$  and energy  $\Delta G_m + a'$  using Eqs (2) and (3) (in which the temperature dependence of the coefficient  $a$  is not considered) for 0.11 mM xanthine solution in 0.2 M NaCl at pH 6 ( $C_0 = 17.7 \mu\text{F cm}^{-2}$ ,  $C_s = 7.1 \mu\text{F cm}^{-2}$ ) and 0.13 mM xanthine in 2 M NaCl at pH 6 ( $C_0 = 18.8 \mu\text{F cm}^{-2}$ ,  $C_s = 7.6 \mu\text{F cm}^{-2}$ ). In Table II, the values calculated using Eqs (14) and (15), with a correction, taking into consideration the dependence of  $a$  on temperature, are presented for the same xanthine solutions.

In Table I it is shown how the results are affected by the chosen value of  $E_m$ . The  $E_m$  value was estimated in several ways:

A) The dependence of the potentials of the anodic and cathodic pit edges  $E_{ha}$ ,  $E_{hc}$  on temperature is, according to Eq. (1), a quadratic function and can be approximated by a parabola<sup>29</sup> (Fig. 8a). This approximation is valid for both the Frumkin and Ising models. The potential  $E_m$  can be defined as the potential at which  $E_{ha} = E_{hc} = E_m$ , the potential of the top of the parabola. This value is given in the column "parabola" of Table I.

B) At  $E = E_m$ , the condensation is fastest;  $E_m$  can be estimated from the  $C-t$  curves and is given in column  $C-t(\text{max})$  in Table I.

C) The potential  $E_m$  is the potential of the minimum of the narrowest capacity pit observed at the highest temperature (column  $\text{pit}(\text{min})$  in Table I).

TABLE I  
Adsorption parameters calculated for 0.11 mM xanthine in 0.2 M NaCl<sup>a</sup> and 0.13 mM xanthine in 2 M NaCl<sup>b</sup> at pH 6 using Eqs (2) and (3)

Parameter	0.2 M NaCl			2 M NaCl		
	parabola	$C-t(\text{max})$	$\text{pit}(\text{min})$	parabola	$C-t(\text{max})$	adsorption potential
$E_m$ , V	-0.561	-0.51	-0.632	-0.614	-0.58	-0.55
$K_1 \cdot 10^{-2}$ $\text{V}^2 \text{K}^{-1}$	$-7.6 \pm 0.1$	$-9.1 \pm 0.2$	$-5.6 \pm 0.1$	$-3.74 \pm 0.07$	$-4.3 \pm 0.1$	$-4.72 \pm 0.09$
$K_2$ , $\text{V}^2$	$2.35 \pm 0.05$	$2.82 \pm 0.06$	$1.71 \pm 0.03$	$1.18 \pm 0.03$	$1.35 \pm 0.03$	$1.50 \pm 0.03$
$\Gamma_m$ , $10^{10}$ $\text{mol cm}^{-2}$	3.7	4.41	2.71	1.94	2.21	2.28
$A$ , $\text{nm}^2$	0.45	0.38	0.61	0.86	0.75	0.73
$\Delta G^m + a'$ $\text{kJ mol}^{-1}$	-33.7	-33.9	-33.5	-34.0	-34.1	-34.2
$T_c$ , K	310	311	307	315	316	318

<sup>a</sup>  $C_0 = 17.7 \mu\text{F cm}^{-2}$ ,  $C_s = 7.1 \mu\text{F cm}^{-2}$ ; <sup>b</sup>  $C_0 = 18.8 \mu\text{F cm}^{-2}$ ,  $C_s = 7.6 \mu\text{F cm}^{-2}$ .

D) In the last column of Table I (column adsorption potential), the potential  $E_m$  was chosen equal to  $-0.55$  V. This value is close to the potential of zero charge measured in  $2$  M NaCl and was used as an adsorption potential during the measurements with double-step technique.

The potential of the anodic pit edge  $E_{ha}$  is, contrary to the cathodic pit edge  $E_{hc}$ , affected by the strong specific adsorption of  $Cl^-$  anions. For the determination of the coefficients  $K_1$  and  $K_2$  according to the Eq. (1), the potential of the cathodic pit edge  $E_{hc}$  was therefore used.

Table I shows that the choice of value  $E_m$  significantly influences the value  $\Gamma_m$  and thus the surface  $A$  occupied by one xanthine molecule in the compact layer:

$$A = 1/(N_a \Gamma_m) , \quad (18)$$

where  $N_a = 6.02 \cdot 10^{23}$  mol $^{-1}$  is Avogadro's number.

Therefore, it is very important to choose the correct value of  $E_m$ . As mentioned earlier, the potential  $E_m$  can be best estimated from the  $C-t$  curves (column  $C-t(\max)$  in Table I). The corresponding values of the surface area  $A$  are  $0.38$  nm $^2$  in  $0.2$  M NaCl and  $0.75$  nm $^2$  in  $2$  M NaCl.

TABLE II  
Adsorption parameters calculated for  $0.11$  mm xanthine in  $0.2$  M NaCl and  $0.13$  mm xanthine in  $2$  M NaCl at pH 6 using Eqs (14) and (15)

Parameter	0.2 M NaCl		2 M NaCl	
	Frumkin	Ising	Frumkin	Ising
$K_1 \cdot 10^{-3}$ , V $^2$ K $^{-1}$	$-9.0 \pm 0.2$		$-4.26 \pm 0.08$	
$K_2$ , V $^2$	$2.82 \pm 0.05$		$1.44 \pm 0.03$	
$K_3 \cdot 10^3$ , K	$7 \pm 0.8$	$3 \pm 0.2$	$4.6 \pm 0.7$	$2.6 \pm 0.3$
$K_4$	$-20 \pm 3$	$-6.1 \pm 0.5$	$-12 \pm 2$	$-5 \pm 1$
$\Gamma_m \cdot 10^{10}$ , mol cm $^{-2}$	$1.72$	$3.01$	$1.14$	$1.60$
$A$ , nm $^2$	$0.97$	$0.55$	$1.46$	$1.04$
$a_c$	$2.0$	$3.53$	$2.00$	$3.53$
$T_c$ , K	$311$	$307$	$321$	$309$
$b$	$10.22$	$1.73$	$6.10$	$1.39$
$a'_c$ , kJ mol $^{-1}$	$-5.2$	$-4.5$	$-5.3$	$-4.5$
$\Delta G^m$ , kJ mol $^{-1}$	$-28.8$	$-25.1$	$-28.3$	$-25.3$
$\Delta G^m + a'_c$ , kJ mol $^{-1}$	$-34.0$	$-29.6$	$-33.6$	$-29.8$

Earlier it was found that adenine in the compact layer occupies about  $0.25 \text{ nm}^2$  (refs<sup>30,31</sup>) or  $0.40 \text{ nm}^2$  (refs<sup>8,32</sup>), which corresponds to the orientation of adenine molecules perpendicular to the electrode surface. Outside the capacity pit region, the area occupied by one molecule is about  $0.60 \text{ nm}^2$  (refs<sup>30,32</sup>) corresponding to the flat-adsorbed adenine molecules. Xanthine molecule has dimensions similar to adenine<sup>33</sup> so that similar values of  $A$  for its planar or perpendicular orientations can be expected. From the  $A$  values given in Table I in column  $C-t(\max)$ , it seems, that in  $0.2 \text{ M}$  NaCl, the perpendicular orientation of condensed molecules is preferred, whereas in  $2 \text{ M}$  NaCl, the planar one. The pit bottom capacity in both electrolytes remains the same (Figs 6 and 7).

The values of the energies ( $\Delta G^m + a'$ ) given in Table I are about  $-34 \text{ kJ mol}^{-1}$  and are not considerably affected by the choice of  $E_m$ . For adenosine in  $0.5 \text{ M}$  KCl at pH 7,  $(\Delta G^m + a') = -22.4 \text{ kJ mol}^{-1}$  (ref.<sup>5</sup>).

Table II summarizes the results calculated using Eqs (14) and (15) (*i.e.*, with the corrected equations (2) and (3) at which the temperature dependence of  $a$  was taken

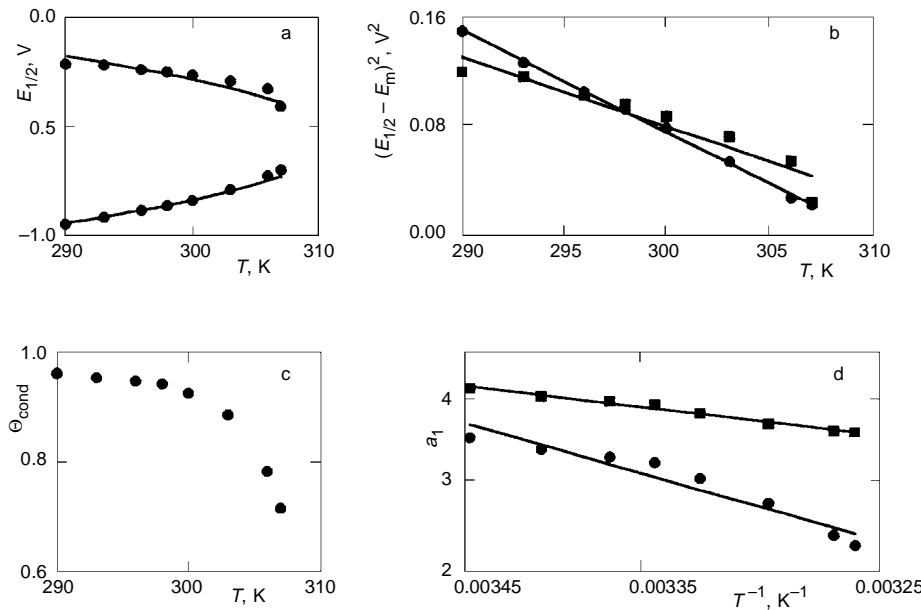


FIG. 8

Temperature dependence of a pit width, b square of the pit half-width, c condensation coverage degree  $\Theta_{\text{cond}}$  and d interaction parameter  $a_1$  for  $0.11 \text{ mm}$  xanthine in  $0.2 \text{ M}$  NaCl, pH 6.0. Solid curves obtained by a fitting; b, c regression. b Edge: ● cathodic, ■ anodic. d Model: ● Frumkin, ■ Ising.  $E_{1/2}$  potential of one pit edge

into consideration) for both the Frumkin and Ising models. From the comparison of Tables I and II, it follows that the  $A$  value is much more affected by this correction than the  $\Delta G^m$  and/or  $(\Delta G^m + a')$  values. The  $A$  values, calculated using a Frumkin isotherm, are even higher than the values which should correspond to the planar orientation of the molecule in both the electrolytes used<sup>35</sup>. Similarly, a relatively high value of  $A$  was found by Retter for 5-iodocytosine in the compact layer,  $A = 1.4 \text{ nm}^2$ . According to Retter<sup>6</sup>, the reason for this could be associated with a linear dependence of  $\Delta G^m$  on temperature not considered in Eq. (15).

The value of interaction energy  $a'_c$  of xanthine in 0.2 M NaCl is very close to that calculated for adenine in ref.<sup>8</sup> ( $-4.7 \text{ kJ mol}^{-1}$ ) and seems to be independent of the NaCl concentration (Table II). The standard Gibbs energy of adsorption,  $\Delta G^m$ , is lower than those found for adenosine ( $\Delta G^m = -15.4 \text{ kJ mol}^{-1}$ , ref.<sup>4</sup>) and adenine ( $\Delta G^m = -13.7 \text{ kJ mol}^{-1}$ , ref.<sup>8</sup>); hence, xanthine is more strongly adsorbed than adenine or adenosine.  $\Delta G^m$  is only little dependent on NaCl concentration.

In order to decide, whether the Frumkin or the Ising model describes better the experimental results the linearity of the  $a$  versus  $T^{-1}$  plot (Fig. 8d) was used as the criterion. According to this criterion, it seems that the adsorption of xanthine can be described better by the Ising model, but the difference between the results of calculation using the Frumkin or Ising models is not large. The 2-D condensation of 5-iodocytosine is better described by Ising model<sup>6</sup> as well, but the difference between descriptions by Ising and Frumkin models was bigger, than in the case of xanthine.

There is evidence for a perpendicular orientation of some other nucleic acid bases and nucleosides in the compact layer at the mercury surface<sup>13,15,30,32</sup>. On the other hand, de Levie and Wandlowski showed that uracil in the compact layer has a planar orientation being stabilized by hydrogen bonds between neighbouring molecules<sup>34</sup>. They have shown that the calculated values of surface  $A$  occupied by one adsorbed molecule are not very convincing for the determination of the orientation of adsorbed molecules at the electrode surface and that some other techniques should be used to complete the electrode impedance measurements for this pursue.

*This work was supported by the Grant Agency of the Academy of Sciences of the Czech Republic (grant No. A 4004702), Grant Agency of the Czech Republic (grant No. 204/97/K 084) and grant KONTAKT No. ES 022 of the Ministry of Education, Youth and Sports of the Czech Republic.*

## REFERENCES

1. Vetterl V.: *Experientia* **1965**, *21*, 9.
2. Vetterl V.: *Collect. Czech. Chem. Commun.* **1966**, *31*, 2105.
3. Vetterl V.: *J. Electroanal. Chem., Interfacial Electrochem.* **1968**, *19*, 169.
4. Vetterl V., de Levie R.: *J. Electroanal. Chem., Interfacial Electrochem.* **1991**, *310*, 305.
5. Retter U., Lohse H.: *J. Electroanal. Chem., Interfacial Electrochem.* **1982**, *134*, 243.
6. Retter U.: *J. Electroanal. Chem., Interfacial Electrochem.* **1984**, *165*, 221.

7. Retter U., Vetterl V., Jursa J.: *J. Electroanal. Chem., Interfacial Electrochem.* **1989**, 274, 1.
8. Sober H. E., Harte R. A. (Eds): *CRC Handbook of Biochemistry*. The Chemical Rubber Co., Cleveland 1968.
9. Sluyters-Rehbach M.: *Ph.D. Thesis*. University of Utrecht, Utrecht 1963.
10. Christensen J. J., Rytting J. H., Izatt R. M.: *Biochemistry* **1970**, 9, 4907.
11. Retter U., Jehring H., Vetterl V.: *J. Electroanal. Chem., Interfacial Electrochem.* **1974**, 57, 391.
12. de Levie R.: *Chem. Rev. (Washington, D. C.)* **1988**, 88, 599.
13. Buess-Herman C.: *Prog. Surf. Sci.* **1994**, 46, 335.
14. Delahay P.: *Double Layer and Electrode Kinetics*, pp. 23, 64. Wiley, New York 1965.
15. Brabec V., Vetterl V., Vrana O. in: *Bioelectrochemistry: Principles and Practice* (V. Brabec, D. Walz and G. Milazzo, Eds), Vol. 3, Chap. 5, p. 287. Birkhäuser Verlag, Basel 1996.
16. Rieger P. H.: *Electrochemistry*, p. 103. Prentice Hall, New Jersey 1987.
17. Miller I. R., Grahame D. C.: *J. Am. Chem. Soc.* **1957**, 79, 3006.
18. Palecek E.: *Electroanalysis* **1996**, 8, 7.
19. Palecek E.: *Anal. Biochem.* **1980**, 108, 129.
20. Ibrahim M. S., Ahmed M. E., Kawde A. M., Temerk Y. M.: *Analysis* **1996**, 24, 6.
21. Ahmed M. E., Ibrahim M. S., Temerk Y. M., Kawde A. M.: *Electrochim. Acta* **1996**, 41, 2883.
22. Rueda M., Mota A., Goncalves M. L. S., Navarro I., Prieto F.: *J. Electroanal. Chem.* **1997**, 431, 257.
23. Francois H., Sharfe M., Buess-Herman Cl.: *J. Electroanal. Chem., Interfacial Electrochem.* **1990**, 296, 415.
24. Scharfe M., Buess-Herman Cl.: *J. Electroanal. Chem.* **1994**, 366, 303.
25. Quarín G.: *Electrochim. Acta* **1984**, 29, 1707.
26. Vetterl V., Papadopoulos N., Sponer J., Mrnustikova P.: Unpublished results.
27. Frumkin A. N. in: *Modern Aspects of Electrochemistry* (J. O'M. Bockris and B. E. Conway, Eds), No. 3, p. 149. Butterworth, London 1964.
28. Retter U.: *J. Electroanal. Chem., Interfacial Electrochem.* **1980**, 106, 371.
29. Sridharan R., de Levie R., Rangarajan S. K.: *Chem. Phys. Lett.* **1987**, 142, 43.
30. Kinoshita H., Christian S. D., Kim M. H., Baker J. G., Dryhurst G.: *ACS Symp. Ser.* **1977**, 38, 113.
31. Jursa J.: *Ph.D. Thesis*. Masaryk University, Brno 1987.
32. Brabec V., Christian S. D., Dryhurst G.: *J. Electroanal. Chem., Interfacial Electrochem.* **1979**, 100, 111.
33. Nonella M., Hanggi G., Dubler E.: *J. Mol. Struct.* **1993**, 279, 173.
34. de Levie R., Wandlowski T.: *J. Electroanal. Chem.* **1994**, 366, 265.
35. Tao N. J., Shi Z.: *Surface Sci.* **1994**, 321, 149.